

# Activation of porous Ni cathodes towards hydrogen evolution by electrodeposition of Ir nuclei

Lourdes Vázquez-Gómez · Sandro Cattarin ·  
Rosalba Gerbasi · Paolo Guerriero ·  
Marco Musiani

Received: 26 September 2008 / Accepted: 18 February 2009 / Published online: 11 March 2009  
© Springer Science+Business Media B.V. 2009

**Abstract** Porous Ni electrodes were modified by electrodeposition of Ir nuclei from  $\text{H}_2\text{IrCl}_6$  solutions at 70 °C, with the aim of activating them towards the hydrogen evolution reaction and comparing their performance with those of porous Ni electrodes activated by spontaneous deposition of noble metals (Ir and Ru). The current efficiency of Ir deposition was found to be very low (1% or lower, decreasing upon increasing deposition current density). Ir deposits characterised by SEM-EDX and XRD consisted of nanocrystals decorating the Ni dendrites forming the porous layers. Ir electrodeposition led to a strong activation of the hydrogen evolution reaction from aqueous 1 M NaOH. The electrocatalytic activity of the cathodes was independent of the Ir deposition charge above the minimum explored value of  $1 \text{ C cm}^{-2}$ . This charge is estimated to correspond to the deposition of ca.  $2.5 \cdot 10^{-8}$  Ir moles  $\text{cm}^{-2}$ . The kinetic parameters for hydrogen evolution were similar for porous Ni electrodes modified by either spontaneous deposition (studied in a previous work) or electrodeposition of Ir.

**Keywords** Cathodic deposition · Electrocatalysis · Porous electrode · Surface roughness

## 1 Introduction

In a recent paper [1] the preparation of Ru-modified and Ir-modified porous Ni electrodes was described. The

Ru-modified electrodes were obtained by combining two procedures described in the literature: the cathodic high rate deposition of porous Ni layers from  $\text{NiCl}_2 + \text{NH}_4\text{Cl}$  mildly acid solutions reported by Marozzi and Chialvo [2, 3] and the spontaneous deposition of Ru onto Ni reported by Dumont et al. [4] and by Bianchi et al. [5]. Ir-modified electrodes were prepared in a comparable way. Thanks to a large surface roughness (defined as the ratio between the true and the geometric electrode area) and to the presence of active noble metal centres, the modified porous Ni electrodes were found to be active as cathodes for the hydrogen evolution reaction [1]. In particular, the Ir-modified electrodes exhibited an exchange current density of the order of  $10 \text{ mA cm}^{-2}$ , a Tafel slope close to  $50 \text{ mV decade}^{-1}$  and an overpotential at  $-100 \text{ mA cm}^{-2}$  as low as  $50 \text{ mV}$  (Ru-modified electrodes were somewhat less active). These results show that spontaneous deposition of noble metals may compare favourably to other methods for the activation of Ni electrodes of high specific surface area [6], like the adsorption of  $\text{Cd}^{2+}$  cations [7], the thermal deposition of  $\text{RuO}_2$  into Raney-Ni micropores [8] and the cathodic co-deposition of  $\text{RuO}_2$  particles with Ni matrices [9–14].

In the present paper we describe the activation of porous Ni layers by cathodic deposition of Ir. Such a procedure was investigated since, in principle, it may offer some advantages with respect to the spontaneous deposition of the noble metal: (i) electrodeposition may be faster than spontaneous deposition and the amount of Ir plated onto porous Ni may be controlled by measuring the deposition charge; (ii) the adhesion between Ir electrodeposits and Ni may be better than the one achieved when Ir spontaneously deposits on a Ni layer which is undergoing a corrosion process; (iii) due to the short duration of the electrodeposition and the polarization of the electrode at negative

L. Vázquez-Gómez · S. Cattarin · M. Musiani (✉)  
IENI CNR, Corso Stati Uniti 4, 35127 Padova, Italy  
e-mail: m.musiani@ieni.cnr.it

R. Gerbasi · P. Guerriero  
ICIS CNR, Corso Stati Uniti 4, 35127 Padova, Italy

potentials, no corrosion of the porous Ni layer, which might induce its partial detachment from the underlying Ni substrate, should be expected. It was reported in Ref. [1] that the spontaneous deposition of Ir (or Ru) was paralleled by a marked increase in the surface area of the porous Ni, which contributed to confer a strong activity to electrode materials thus obtained. Being due to the corrosion of the Ni deposits, such a surface area increase cannot be expected as a result of Ir electrodeposition.

The cathodic electrodeposition of Ir is a difficult process, because the concomitant hydrogen evolution, catalysed by the Ir deposits themselves, severely limits its current efficiency [15–17]. According to McNamara [15], a current efficiency as high as 14% can be obtained with an appropriate choice of the critical operating parameters, i.e. concentration of the Ir complex ion, current density and temperature which must be higher for lower Ir ion concentration and generally well above room temperature. However, dramatically lower current efficiencies, in the range 0.05% [17] to 0.8% [16] were reported by other workers.

## 2 Experimental

### 2.1 Equipment and materials

Porous Ni layers, and successively Ir, were deposited onto Ni disc electrodes ( $0.34\text{ cm}^2$  geometric area) and Ni sheet electrodes ( $2\text{ cm}^2$ ); all current densities were calculated dividing the current by these geometric areas, regardless of the electrode surface roughness. Prior to use, the Ni electrodes were polished with emery paper 1,000, rinsed with water and dried in air. Sheet electrodes were used in the tests aimed at determining the current efficiency of Ir electrodeposition and for SEM-EDX and XRD characterization; the disc electrodes were used in all the other experiments.

Porous Ni electrodeposition was performed in a cell consisting of a main central cylindrical compartment, where the working electrode was positioned, connected through glass frits to two lateral compartments where two Ni wire counterelectrodes (overall area  $2\text{ cm}^2$ ) were placed. The disc electrodes were rotated at 2,500 revolutions per minute, so as to remove hydrogen bubbles formed in a side reaction. Ir electrodeposition was performed in a two-compartment cell. The disc electrode, previously coated with porous Ni, was positioned in the main compartment, with the electrode/electrolyte interface placed vertically, so as to facilitate the release of the hydrogen bubbles produced. A Pt wire in the same compartment was used as counter electrode. An SCE was used as reference and placed in the lateral compartment connected to the

main one through a Luggin capillary. The same cell was used in the characterization of the Ir-modified porous Ni electrodes by cyclic voltammetry and in the study of their activity in hydrogen evolution. An Hg/HgO/5 M KOH reference electrode was used for hydrogen evolution experiments in basic solutions. All potentials mentioned in the present paper are referred to Hg|HgO|5 M KOH electrode. The potential of the cell  $\text{H}_2, \text{Pt}|\text{KOH}_{(\text{aq})}|\text{HgO}|\text{Hg}$  was reported to be 0.9265 V [18].

The electrochemical equipment consisted of either an AMEL Model 2053 potentiostat or an Autolab PGSTAT 100. SEM analyses were performed with a FEI Quanta 200 FEG ESEM instrument, equipped with a field emission gun, operating in high vacuum condition at an accelerating voltage variable from 5 to 30 keV, depending on the observation needs. EDX analyses were obtained by using an EDAX Genesis energy-dispersive X-ray spectrometer at an accelerating voltage of 25 keV. X-Ray Diffraction (XRD) patterns were obtained by using a Philips X-PERT PW3710 diffractometer with a Bragg-Brentano geometry, employing a  $\text{CuK}\alpha$  source (40 kV, 30 mA).

### 2.2 Procedures

Porous Ni layers were deposited from 0.2 M  $\text{NiCl}_2 + 2\text{ M NH}_4\text{Cl}$  aqueous solutions, pH 4.5, kept at 25 °C, under galvanostatic control [2, 3]. Typically a current density of  $-1.0\text{ A cm}^{-2}$  was applied for 60 s, so as to obtain a deposition charge density of  $60\text{ C cm}^{-2}$  which, taking into account the current efficiency of Ni deposition [13] and neglecting the pores volume, corresponds to a Ni layer thickness of ca. 20  $\mu\text{m}$ . The Ni deposits surface roughness is expected to be in the range 10–20. Once removed from the deposition bath, the Ni deposits were carefully rinsed with water, dried and transferred to the Ir electrodeposition solution.

The electrodeposition of Ir was carried out from deaerated  $2 \cdot 10^{-3}\text{ M H}_2\text{IrCl}_6$  solutions, pH ca. 2.5, generally kept at 70 °C with a thermostat. 0.5 M NaCl was used as supporting electrolyte in some preliminary cyclic voltammetry experiments. Ir electrodeposition was carried out at constant current density, generally in the range between  $-2$  and  $-20\text{ mA cm}^{-2}$ . The working electrode, once dipped in the Ir ion solution, was immediately polarized at negative potential; therefore, spontaneous deposition of Ir was negligible, considering the slow rate of this process [1].

Current efficiency was estimated after prolonged galvanostatic electrolyses at two different current densities, from the charge transferred during electrodeposition and the mass increase of Ni sheet electrodes.

As-deposited and Ir-modified porous Ni electrodes were submitted to the following sequence of electrochemical

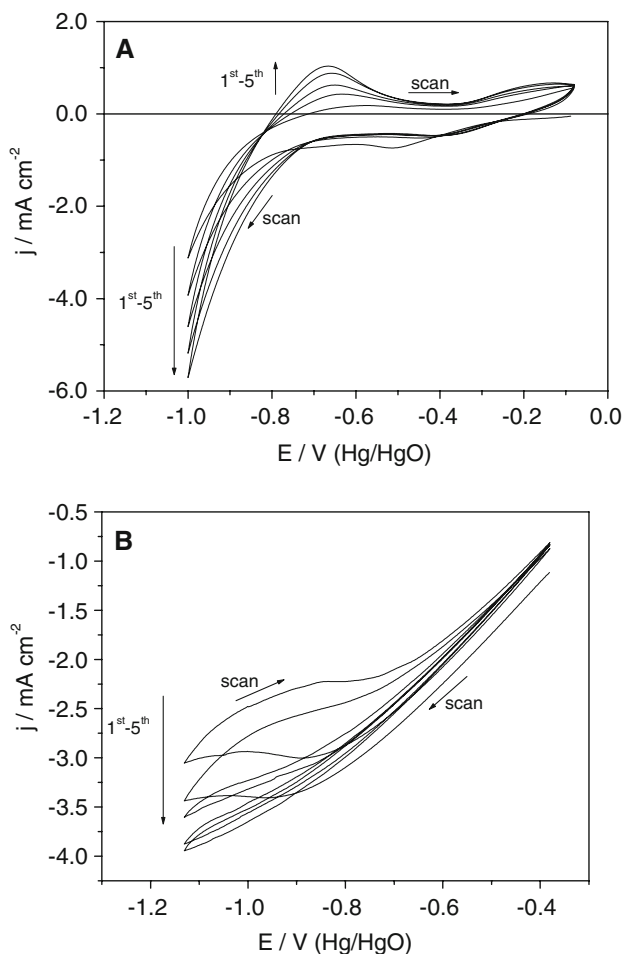


**Fig. 1** Cyclic voltammograms obtained at Ni electrodes in deaerated  $2 \times 10^{-3}$  M  $\text{H}_2\text{IrCl}_6$  solution, at  $50 \text{ mV s}^{-1}$ . **a** polished Ni disc electrode; the solution contained 0.5 M NaCl supporting electrolyte and was kept at  $25^\circ\text{C}$ . **b** Porous Ni disc electrode; the solution devoid of supporting electrolyte was kept at  $70^\circ\text{C}$ . Scan direction and cycles succession are indicated by arrows on the figure

tests in 1 M NaOH aqueous solutions, at  $25^\circ\text{C}$ : (i) at first, a steady-state current potential curve was recorded to study the hydrogen evolution reaction; (ii) the electrode was polarized in the hydrogen evolution region for 10 minutes and three successive cyclic voltammograms were recorded in the range where hydrogen underpotential deposition and desorption is expected; (iii) five successive cyclic voltammograms were recorded to study the Ni(II)/Ni(III) reaction taking place at the electrode surface [19, 20]; (iv) a final steady-state current potential curve was recorded under the same conditions as in step (i). Tafel plots were obtained from the steady-state current potential curves, after correction of the ohmic drop; the values of the electrolyte resistance used for the correction were determined by EIS, as the high frequency limit of the real part of the impedance.

### 3 Results and discussion

#### 3.1 Preparation and characterization of Ir-modified porous Ni electrodes

##### 3.1.1 Cyclic voltammetry

Figure 1a shows five successive cyclic voltammograms recorded with a polished Ni disc electrode in deaerated  $2 \times 10^{-3}$  M  $\text{H}_2\text{IrCl}_6 + 0.5$  NaCl solution, at  $25^\circ\text{C}$ . The progressive increase of the cathodic current in the successive cycles provides a hint that Ir is being deposited and catalyses hydrogen evolution (and possibly further Ir deposition). Consistently, the height of the anodic peak due to hydrogen

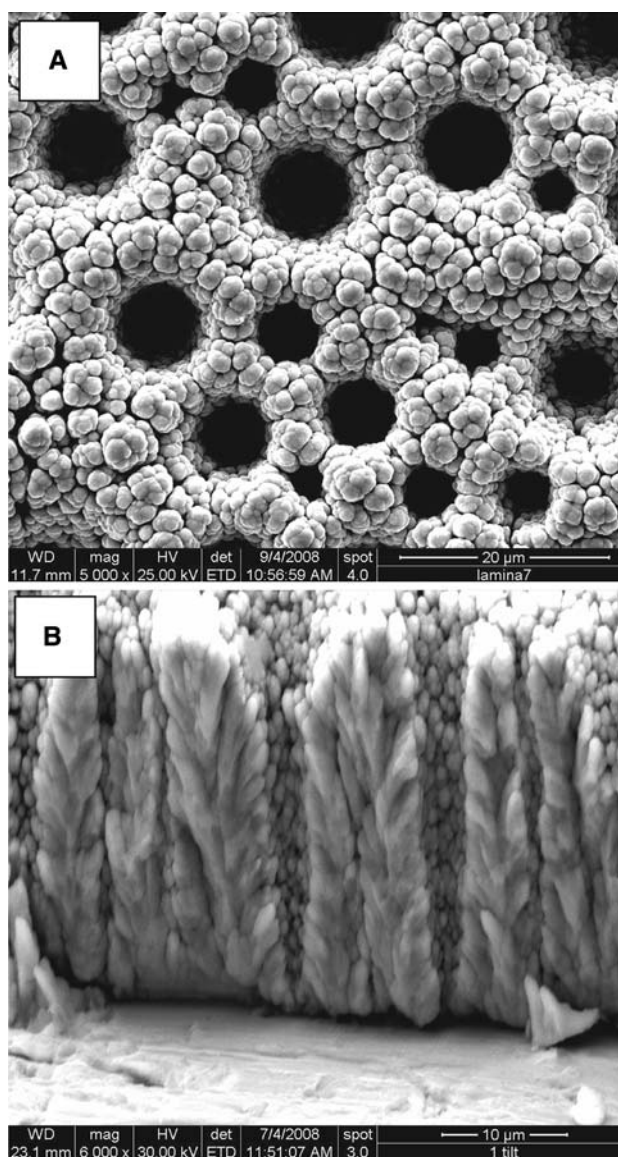


**Fig. 2** Morphology of porous Ni deposits grown onto Ni sheet electrodes. **a** outer surface of the deposit; **b** fracture surface



**Fig. 3** Ir deposits formed onto Ni substrates from deaerated  $2 \cdot 10^{-3}$  M  $\text{H}_2\text{IrCl}_6$  solution, at  $70^\circ\text{C}$ . **a** Ir deposit formed onto bulk Ni polished with abrasive paper; electrolyses at  $-2 \text{ mA cm}^{-2}$  for 15 h. **b** Ir deposit formed onto porous Ni; electrolyses at  $-2 \text{ mA cm}^{-2}$  for 15 h. **c** Ir deposit formed onto porous Ni; electrolyses at  $-20 \text{ mA cm}^{-2}$  for 0.5 h

desorption increases. A comparable but faster evolution was observed at  $70^\circ\text{C}$ . A similar increase of the cathodic current with the successive cycles is observed in Fig. 1b, relevant to a porous Ni electrode immersed in an NaCl free  $2 \cdot 10^{-3}$  M  $\text{H}_2\text{IrCl}_6$  solution, at  $70^\circ\text{C}$ , where the voltammetric curves are severely distorted by ohmic resistance, in spite of the high temperature. The latter solution was used in galvanostatic electrolyses aimed at modifying porous Ni electrodes, as it was similar to the conditions recommended in Ref. [15].

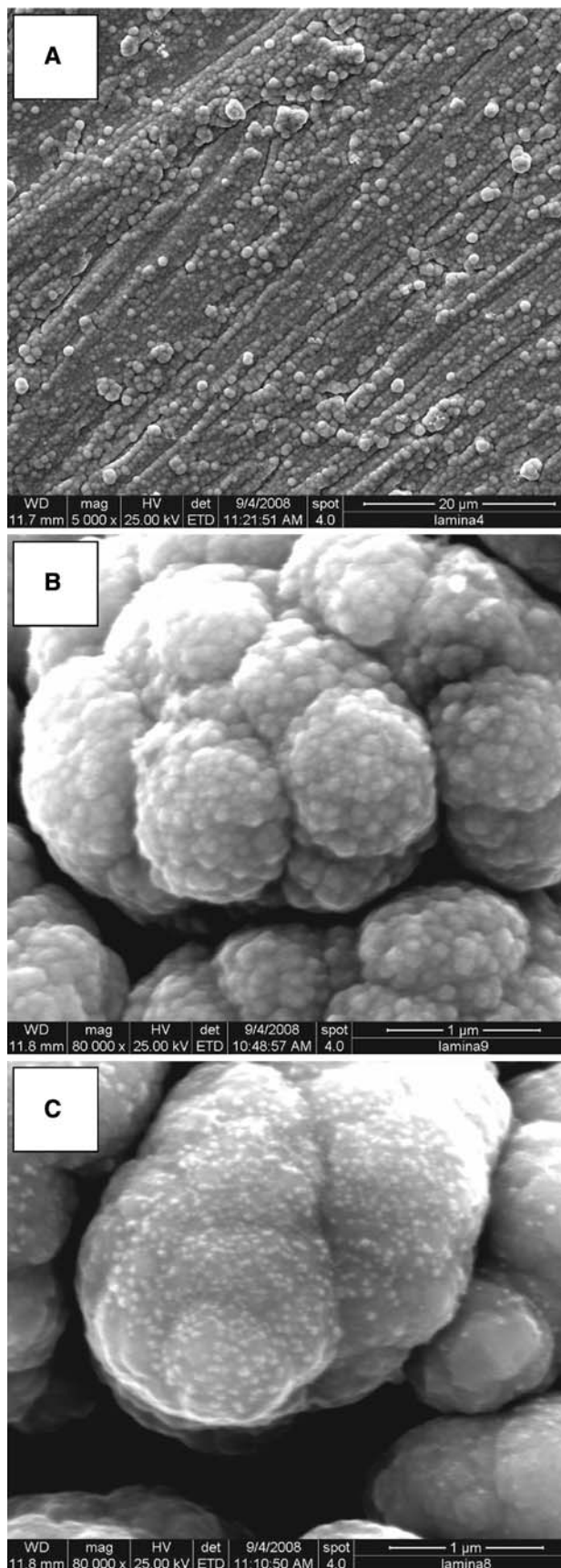
### 3.1.2 Current efficiency

In order to measure the current efficiency of Ir deposition, polished Ni sheet electrodes were used as cathodes, with deposition current densities of either  $-2$  or  $-20 \text{ mA cm}^{-2}$  and electrolyses duration up to 2 h at the higher current and up to 15 h at the lower one. Significantly shorter experiments did not allow a reasonably accurate measurement of the electrode mass increase. Current efficiencies were found to be 0.9 to 1% at  $-2 \text{ mA cm}^{-2}$  and close to 0.3% at  $-20 \text{ mA cm}^{-2}$ , i.e. much lower than reported by McNamara [15] and similar to, or somewhat higher than those reported by other groups [16, 17].

### 3.1.3 SEM-EDX and XRD characterization

Figure 2 shows the morphology of porous Ni deposits grown onto Ni sheet electrodes. Part A shows a large density of deep and large pores, with typical diameters in the range 5 to  $15 \mu\text{m}$ . The image of a fracture section (part B) shows that these large pores often extend over the whole deposit thickness. This morphology results from hydrogen bubbles trapped within the growing deposit and from a preferential growth in the direction perpendicular to the electrode surface. In comparison, deposits grown onto rotating disc electrodes showed less numerous and less deep large pores, due to efficient bubble removal (see images in Refs. [1, 13, 21]). Figure 2 also shows the dendritic structure of the Ni deposits and the extensive presence of narrow pores of irregular shape, with lateral dimension of the order of or lower than  $1 \mu\text{m}$ , which separate the dendrites.

Figure 3a shows the morphology of an Ir deposit obtained after prolonged electrolysis (15 h at  $-2 \text{ mA cm}^{-2}$ ;  $108 \text{ C cm}^{-2}$  deposition charge) onto a Ni sheet substrate. A continuous layer consisting of Ir nodules covers the whole



electrode. Figure 3b shows, with a much larger magnification, the Ir deposit obtained under comparable conditions onto a porous Ni substrate. The Ni dendrites are homogeneously coated by a nodular Ir deposit. As far as it can be seen in the SEM images, Ir deposition is not limited to the dendrites top. No filling of the gaps separating the dendrites is observed even after prolonged Ir deposition. Figure 3c shows a sample obtained with a shorter electrolysis time and a higher current density (1,800 s at  $-20 \text{ mA cm}^{-2}$ ;  $36 \text{ C cm}^{-2}$  deposition charge): the Ni dendrites are decorated by a large number of Ir nuclei, with a typical dimension of 100 nm or lower, and no continuous Ir layer is detected. SEM images of samples obtained by transferring charges ca. 10 times lower, at either current density ( $-2$  or  $-20 \text{ mA cm}^{-2}$ ) failed to show Ir deposits.

The samples shown in Fig. 3a and 3b were submitted to an XRD analysis. Their diffractograms are shown in Fig. 4 and compared to the lines expected for Ni and Ir, respectively. In both cases the most intense peaks can be ascribed to Ni, but Ir peaks are also visible, although they are systematically shifted towards higher  $2\theta$  values. Such a shift, which cannot be an experimental artifact since the Ni peaks are not equally shifted, probably corresponds to cell dimensions lower than normal, possibly due to compressive stress of the deposits. By applying the Scherrer formula, the average Ni crystallite size may be estimated to be ca. 25 nm for the porous Ni deposit, as compared to ca. 90 nm for bulk Ni; on both substrates the Ir crystallites size is of the order of 4 nm.

The samples shown in Fig. 3b and 3c were submitted to EDX analyses. The corresponding spectra are shown in Fig. 5 (the spectra are normalized with respect to the NiK $\alpha$  peak and shifted along the ordinate axis, for clarity). The Ir peaks are clearly visible in the upper spectrum, but they are just above the detection limit in the lower one, as a result of the combined effects of a 3 times lower deposition charge and a ca. 3 times lower current efficiency. No unambiguous Ir peak could be seen for samples obtained with significantly lower deposition charges, e.g. 1 to  $10 \text{ C cm}^{-2}$ .

### 3.2 Electrochemical behaviour of Ir-modified porous Ni electrodes and hydrogen evolution from 1 M NaOH

It was shown in Ref. [1] that the spontaneous deposition of Ir (or Ru) caused a marked increase in the surface area of porous Ni, witnessed by the increase in the charge associated to the NiOOH/Ni(OH) $_2$  redox couple at the electrode surface, found in the potential range 0.35 to 0.55 V. Cyclic voltammeteries recorded in the same potential range on porous Ni electrodes modified by electrodeposition of Ir at  $-20 \text{ mA cm}^{-2}$ , with deposition charges up to  $16 \text{ C cm}^{-2}$ , showed only minor variations in the NiOOH/Ni(OH) $_2$  redox

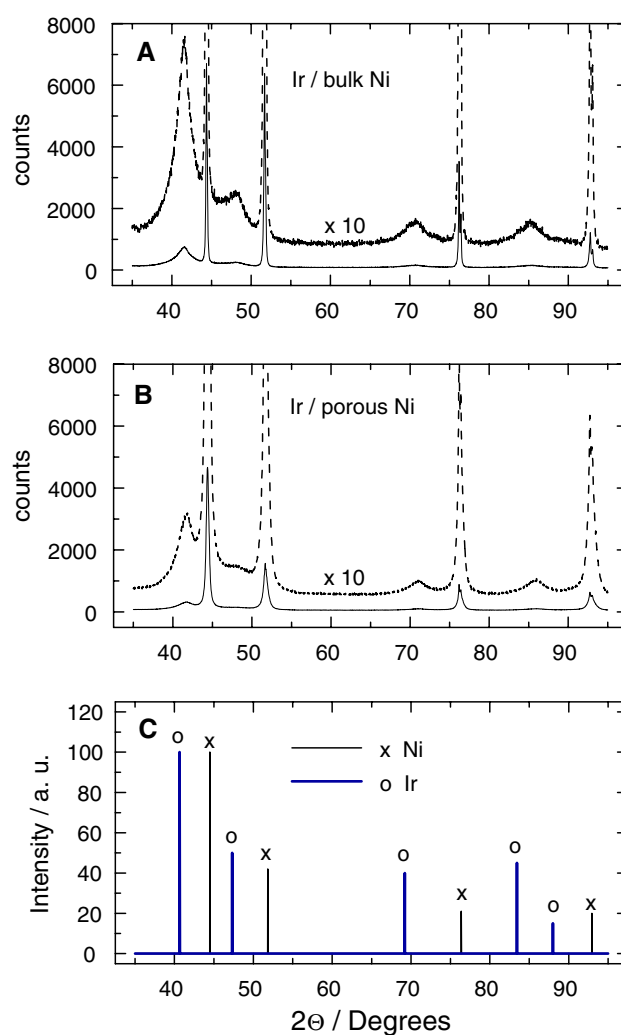


**Fig. 4** X-ray diffractograms of Ir deposits formed either onto bulk Ni polished with abrasive paper (a) or onto porous Ni (b) by electrolysing at  $-2 \text{ mA cm}^{-2}$  for 15 h in  $2 \cdot 10^{-3} \text{ M H}_2\text{IrCl}_6$  solution, compared with ICDD patterns of (c): Ir, ICDD card 06-0598; Ni, ICDD card 04-0850

charge, comparable to the dispersion of redox charges measured on nominally identical porous Ni electrodes.

The cyclic voltammeteries recorded in the potential range of hydrogen underpotential deposition and desorption, at porous Ni electrodes modified by either spontaneous deposition or electrodeposition at two current densities, are compared in Fig. 6: very similar currents are measured in all cases. The shape and size of these curves changed very little with the Ir deposition duration and current density. Therefore, no attempt was made to use the voltammetric charges to quantify the amount of Ir electrodeposited. At potentials less negative than  $-0.8 \text{ V}$ , the current is significantly higher for the electrode modified by spontaneous deposition than for those modified by electrodeposition. The most probable reason is the larger surface area of the

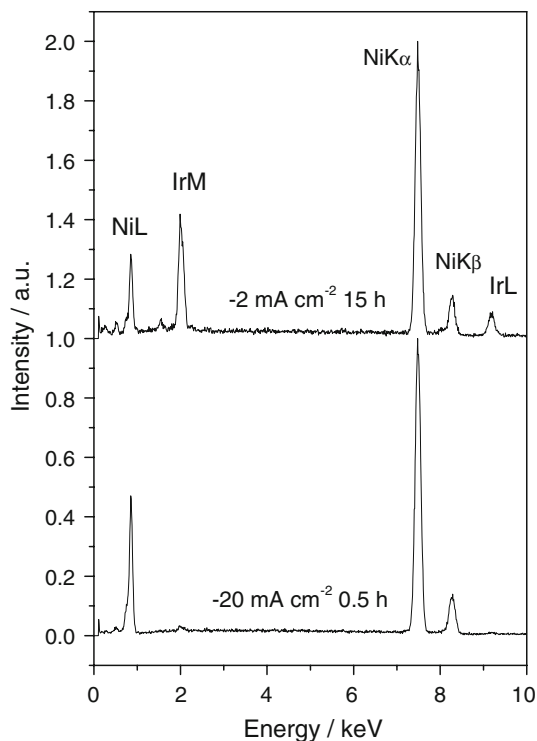


**Fig. 5** EDX spectra of Ir deposits formed onto porous Ni; electrolyses at  $-2 \text{ mA cm}^{-2}$  for 15 h (top) or at  $-20 \text{ mA cm}^{-2}$  for 0.5 h (bottom) in  $2 \cdot 10^{-3} \text{ M H}_2\text{IrCl}_6$  solution

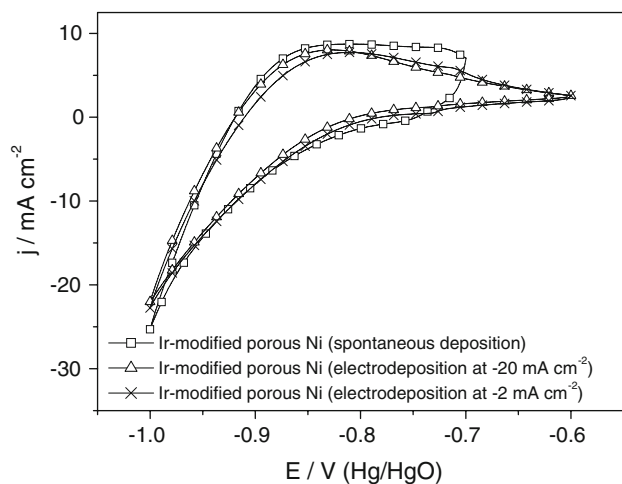


**Fig. 6** Cyclic voltammograms (in the potential range of hydrogen underpotential deposition and desorption) recorded at porous Ni electrodes modified by either Ir spontaneous deposition or Ir electrodeposition at two current densities indicated on the figure. Electrolyte:  $1 \text{ M NaOH}$ . Scan rate:  $10 \text{ mV s}^{-1}$

former, due to Ni corrosion accompanying Ir deposition [1], and a correspondingly higher double layer capacity.

Figure 7 shows Tafel plots for the hydrogen evolution reaction from  $1 \text{ M NaOH}$ : porous Ni is compared to electrodes modified by Ir spontaneous deposition (6 h treatment) [1] or by Ir electrodeposition at two current densities ( $-2$  and

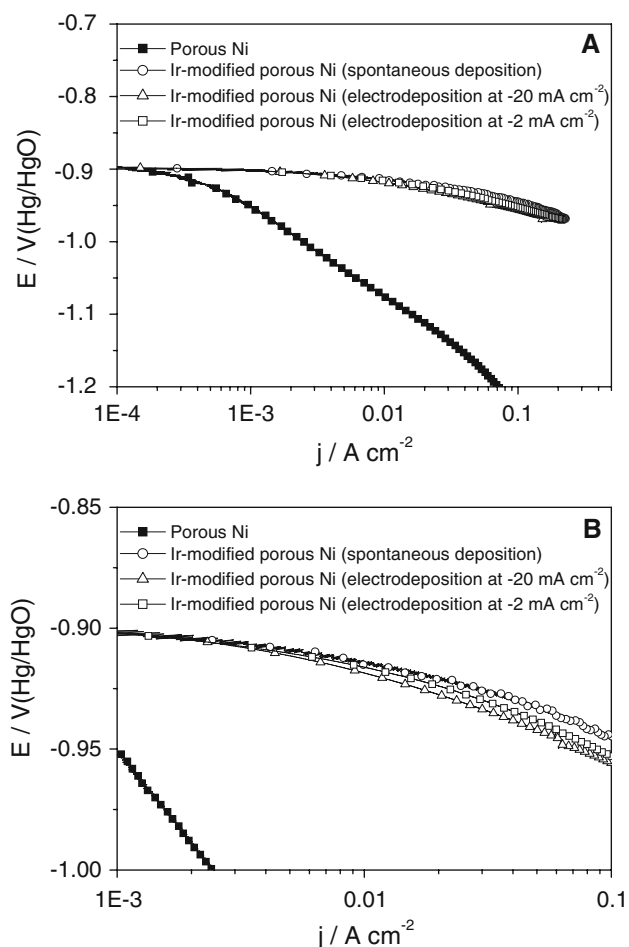


**Fig. 7** Tafel plots of the current-potential curves recorded at Ir-modified porous Ni electrodes, in  $1 \text{ M NaOH}$ . Ir deposition was carried out by simple immersion for 2 h or by electrodeposition in  $\text{H}_2\text{IrCl}_6$  solution, as indicated on the figure. As-deposited porous Ni is shown for comparison. Part B is an enlarged view of part A

$-20 \text{ mA cm}^{-2}$ ). Part A clearly shows that all treatments strongly activate the porous Ni. Part B allows to better appreciate the more subtle differences between the spontaneous and the electrochemical deposition. Both Tafel slopes (close to  $50 \text{ mV decade}^{-1}$ , in the range of large currents) and the overpotential at an arbitrary  $-100 \text{ mA cm}^{-2}$  current density are similar in all cases. The electrode modified by spontaneous deposition is somewhat better than those bearing Ir electrodeposits, possibly because of its larger surface roughness. The lower Ir deposition current density ( $-2 \text{ mA cm}^{-2}$ ) produces slightly more active electrodes than the higher one ( $-20 \text{ mA cm}^{-2}$ ). This result is not surprising since the Ir deposition charge is similar for both electrodes, the current efficiency decreases significantly upon increasing the deposition current density, and thus the Ir loading is expected to be higher the lower is the deposition current density.

The electrode potential necessary to sustain a current density of  $-100 \text{ mA cm}^{-2}$  is plotted in Fig. 8 as a function

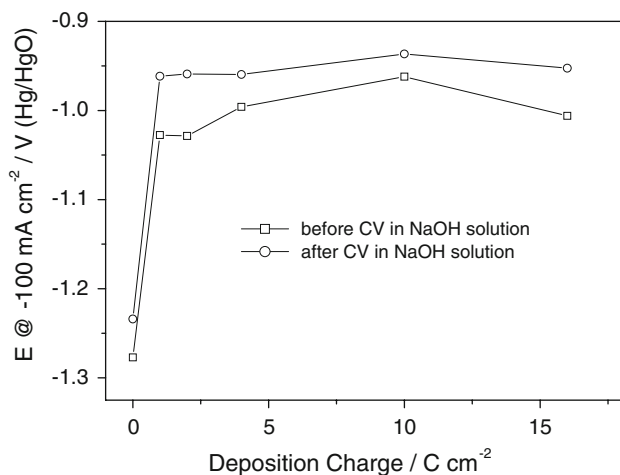


**Fig. 8** Dependence of the cathode potential necessary to sustain hydrogen evolution from 1 M NaOH at  $-100 \text{ mA cm}^{-2}$  on the charge spent in the deposition of Ir onto porous Ni electrodes (deposition current density  $-20 \text{ mA cm}^{-2}$ )

of the charge spent for depositing Ir, at a current density of  $-20 \text{ mA cm}^{-2}$ . Clearly, the enhancement of the catalytic activity of the electrode is achieved with a deposition charge as low as  $1 \text{ C cm}^{-2}$ , corresponding to an electrolysis duration of 50 s. Longer electrolyses do not further increase the activity. Assuming that the current efficiency measured in prolonged electrolyses at polished Ni is the same as that obtained, in the early deposition stages, at porous Ni, the amount of Ir deposited during 50 s can be estimated to be ca.  $5 \cdot 10^{-6} \text{ g cm}^{-2}$ , i.e. ca.  $2.5 \cdot 10^{-8} \text{ moles cm}^{-2}$ . These figures are almost certainly underestimated since the same nominal current density (referred to geometric area) corresponds to a 10–20 times lower true current density at porous Ni than at polished Ni, and therefore a 3–5 times higher current efficiency might be expected for the former. Even in this case, comparison of electrochemical, SEM, EDX and XRD data shows that the limiting activation is already induced by Ir deposits of such a small mass that they are neither visible in SEM images, nor detectable by EDX or XRD.

Comparison of the plots in Fig. 8 obtained before and after cycling the Ir-modified electrodes in the Ni(II)/Ni(III) range, shows that these electrodes are activated by oxidation, as already observed in our study of porous Ni electrodes activated by spontaneous deposition of noble metals [1] and for Ni electrodes in previous studies [22].

#### 4 Conclusions

A study on the activation of porous Ni cathodes towards the hydrogen evolution reaction by electrodeposition of Ir nuclei, in comparison with the activation achieved by spontaneous deposition [1], was carried out.

Ir-modified porous Ni electrodes active in the hydrogen evolution reaction from basic media were obtained by two successive electrodeposition stages: in the first, porous Ni layers consisting of Ni dendrites were obtained from  $\text{NiCl}_2 + \text{NH}_4\text{Cl}$  solutions [2,3]; in the second, Ir nuclei decorating the Ni dendrites were deposited in warm  $\text{H}_2\text{IrCl}_6$  solutions [15].

Despite the low current efficiency of the Ir deposition process, active electrodes were produced by electrolyses lasting less than 1 min, since an Ir loading as low as  $5 \cdot 10^{-6} \text{ g cm}^{-2}$ , i.e. ca.  $2.5 \cdot 10^{-8} \text{ moles cm}^{-2}$ , ensured good performance. A marked shortening of the preparation process is the main advantage of electrodeposition, with respect to spontaneous deposition. However, spontaneous deposition produced slightly more active cathodes, most probably due to the increase in Ni surface roughness taking place at open circuit under the effect of the oxidizing action of Ir(IV) complex ions [1].

SEM-EDX and XRD were ineffective in the characterization of Ir-modified electrodes with very low Ir loading. Samples prepared by transferring electrolytic charges 30 to 100 times higher than that necessary to achieve full electrochemical activation were shown to consist of assemblies of Ni dendrites, still retaining the morphology of as-deposited porous Ni deposits, decorated by Ir nanocrystals which progressively coated the Ni as the deposition charge was increased.

**Acknowledgments** The authors are indebted to FILA INDUSTRIA CHIMICA SPA, San Martino di Lupari, Padova, Italy, owner of the Fei-ESEM FEI Quanta 200 FEG instrument, for allowing its use for the research work described in this article.

#### References

- Vázquez-Gómez L, Cattarin S, Guerriero P, Musiani M (2008) *Electrochim Acta* 53:8310
- Marozzi CA, Chialvo AC (2000) *Electrochim Acta* 45:2111
- Marozzi CA, Chialvo AC (2001) *Electrochim Acta* 46:861
- Dumont H, Los P, Lasia A, Menard H, Brossard L (1993) *J Appl Electrochem* 23:684
- Bianchi I, Guerrini E, Trasatti S (2005) *Chem Phys* 319:192
- Trasatti S (1992) Electrocatalysis of hydrogen evolution: progress in cathode activation. In: Gerischer H, Tobias CW (eds) *Advances in electrochemical science and engineering*, vol 2. VCH, Weinheim, p 1
- Korovin NV, Udriș EYa, Savel'eva ON (1986) *Sov Electrochem* 23:330
- Shervedani RK, Kazemi SH, Lasia A, Mehrjerdi HRZ (2005) *J New Mat Electrochem Sys* 8:213
- Iwakura C, Furukawa N, Tanaka M (1992) *Electrochim Acta* 37:757
- Iwakura C, Tanaka M, Nakamatsu S, Noue H, Matsuoka M, Furukawa N (1995) *Electrochim Acta* 40:977
- Miousse D, Lasia A (1999) *J New Mat Electrochem Syst* 2:71
- Tavares AC, Trasatti S (2000) *Electrochim Acta* 45:4195
- Vázquez-Gómez L, Cattarin S, Guerriero P, Musiani M (2007) *Electrochim Acta* 52:8055
- Antozzi AL, Bargioni C, Iacopetti L, Musiani M, Vázquez-Gómez L (2008) *Electrochim Acta* 53:7410

15. MacNamara EL (1962) *J Electrochem Soc* 109:61
16. Llopis JF, Colom F (1976) In: Bard AJ (ed) *Encyclopedia of the electrochemistry of the elements*, vol VI. Marcel Dekker, New York, p 221
17. Čukman D, Vuković M (1990) *J Electroanal Chem* 279:283
18. Ives DJG (1961) In: Ives DJG and Janz GJ (eds) *Reference electrodes. Theory and practice*. Academic Press, New York, p 335
19. Sattar MA, Conway BE (1969) *Electrochim Acta* 14:695
20. Schrebler Guzman RS, Vilche JR, Arvia AJ (1978) *J Electrochem Soc* 125:1578
21. Huet F, Musiani M, Nogueira RP (2004) *J Solid State Electrochem* 8:786
22. Lasia A, Rami A (1980) *J Electroanal Chem* 294:123